New insights into the interactions between electrode materials and electrolyte solutions for advanced nonaqueous batteries

D. Aurbach *, B. Markovsky, M.D. Levi, E. Levi, A. Schechter, M. Moshkovich, Y. Cohen

Department of Chemistry, Bar-Ilan University, Ramat-Gan 52900, Israel

Abstract

In this paper we review some recent work with Li metal and Li–graphite anodes and Li_xMO_y cathodes (M = transition metals such as Ni, Co, Mn). The emphasis was on the study of surface phenomena using in situ and ex situ FTIR spectroscopy, atomic force microscopy (in situ AFM), electrochemical quartz crystal microbalance (EQCM) and impedance spectroscopy (EIS). The performance of Li metal and Li–carbon anodes in secondary batteries depends on the nature of the surface films that cover them. The use of Li metal anodes requires the formation of highly uniform and elastic surface films. Thus, most of the commonly used liquid electrolyte solutions are not suitable for Li metal-based rechargeable batteries. In the case of Li–C-based batteries, the passivating films need not be elastic. Channeling the Li–C electrode surface chemistry towards the formation of Li_2CO_3 surface films provides adequate passivation for these electrodes. This can be achieved through the use of EC-based solutions of low EC concentration (cosolvents should be less reactive than EC). An interesting finding is that the behavior of many commonly used cathodes also depends on their surface chemistry, and that their overall Li insertion processes include the step of Li ion migration through surface films. Their origin is discussed herein, as well as possible oxidation processes of the relevant solutions. © 1999 Elsevier Science S.A. All rights reserved.

1. Introduction

During the last few years, rechargeable Li batteries became a commercial reality. There are rechargeable Li metal anode-based batteries [1] and a variety of rechargeable Li-ion batteries on the market [2]. We should note, however, that these commercially available rechargeable high energy density battery systems are products of more than three decades of intensive worldwide research efforts. It should be emphasized that R&D of Li batteries requires an intensive investment in basic science, since the materials involved (anodes, cathodes, electrolyte systems) are reactive and highly sensitive to the atmospheric components and to each other, and the electrode–electrolyte interactions are very complicated. A partial list of such complications appears below.

(1) Surface films that control their electrochemical behavior cover all the electrodes in Li batteries (Li metal, lithiated carbons, lithiated transition metal oxides).

(2) The structure of these surface films is complicated. They are multi-layered and microscopically non-uniform (mosaic-like). Thus, they may lead to highly non-uniform processes of Li dissolution–deposition in the case of Li metal anodes, or Li insertion–deinsertion when the electrodes are lithiated carbons and transition metal oxides.

(3) Although Li or Li–C electrodes are usually passivated by surface films in the optimized electrolyte solutions, continuous reactions between the active electrodes and solution species remain unavoidable. Thereby, the cycle life of Li and Li–carbon-based anodes is always limited because of slow degradation of both the electrolyte solutions and the anodes' active mass.

(4) The problems related to the high reactivity of Li and Li–C towards liquid electrolyte solutions led to extensive attempts to develop solid polymeric-based electrolytes for Li and Li ion batteries. In spite of the great success achieved to date in R&D of polymeric electrolyte systems for Li batteries, there are still problems of conductivity, contact with the electrodes and stability that have to be overcome.

(5) Most types of Li batteries are based on Li insertion electrodes in which Li intercalates and deintercalates repeatedly. These processes involve periodic volume changes of the host materials. Thus, we often find that Li insertion electrodes such as Li–C anodes or Li_xMO_y cathodes

---

* Corresponding author. Tel.: +972-3-531-8317; Fax: +972-3-535-1250; E-mail: aurbach@mail.biu.ac.il

(M = transition metal such as Mn, Co, Ni, V, etc.) are not fully stable upon charge–discharge cycling. Unavoidable structural changes that reduce the capacity and slow down the kinetics of these electrodes may occur.

The above listed complications require rigorous studies of interfacial phenomena, as well as investigation of the correlation between the electrodes' structure and morphology, and their basic electrochemical behavior.

In spite of the impressive development of commercial rechargeable Li batteries in recent years, there is still a long way to go with these battery systems in terms of long cycle life at steady capacity, minimal self-discharge, wide temperature range of operation and the possibility of up-scaling Li batteries to large systems (for applications such as electric vehicles). The development of surface sensitive analytical techniques in recent years, in situ spectroanalytical techniques in particular, has opened the door for an efficient and detailed study of the correlation amongst surface chemistry, morphology, 3D structure, and the electroanalytical response and performance of electrodes and electrolyte systems for advanced Li batteries. Such a study is a prerequisite for improving existing Li battery systems and the development of more advanced systems.

The aim of this paper is to review some of our own recent studies of electrode–solution interactions with the emphasis on the use of spectroelectrochemical tools in conjunction with combined electroanalytical techniques.

2. Experimental considerations

We studied the surface chemistry of Li electrodes using in situ and ex situ FTIR spectroscopy, XPS and EDAX, as already reported [3,4]. The surface chemistry of Li–C and Li_xMO_y (M = transition metal) electrodes was also studied using diffuse reflectance mode [4]. In this method, pristine electrode materials, pristine electrode composites and electrode particles scraped from the electrode after any desired electrochemical process, are measured comparatively ex situ in a powder form. The FTIR spectrometer was placed in a glove box, and thus the measurements could be conducted with no detrimental interaction with active atmospheric gases.

The morphology of Li electrodes was studied by in situ atomic force microscopy, as already described [5]. The structural changes of Li insertion electrodes was studied by in situ and ex situ XRD, as already reported [6]. The electrochemical behavior of electrodes in solutions was studied by combined simultaneous application of chronopotentiometry, fast and slow scan rate cyclic voltammetry (SSCV), potentiostatic intermittent titration (PITT) and impedance spectroscopy (EIS). The technical details were reported in Refs. [7,8].

The simultaneous use of in situ FTIR and impedance spectroscopies, AFM and electrochemical quartz crystal microbalance (EQCM) was found to be highly useful for the study of surface film formation processes on electrodes in solutions of interest and for studying the stability of the surface species [9,10]. The preparation of composite Li–C and Li_xMO_2 electrodes was already described [7,8,11]. We used highly pure solvents from Merck and Tomiyama, and Li salts from Hashimoto, Merck, and Tomiyama. Li_xMO_y cathode materials were obtained from Merck.

3. Results and discussion

3.1. General

The strategy of our research is schematically sketched in Fig. 1. The theme of our studies is the use of as many sources of information as possible in a single study, and the simultaneous attack of problems related to Li, Li–C and $LiMO_x$ (M = transition metal, including Mn, Co, Ni and V). A key issue is the investigation of the correlation among surface chemistry, morphology and 3D structure, electronic properties, basic electroanalytical responses and the practical performance of the various electrodes in a large variety of solvents, salts and additives. As shown in Fig. 1, an important source of information results from a rigorous and systematic study of non-active metal electrodes (e.g., Pt, Au, Ni). We discovered that non-active metal electrodes, when polarized to low potentials, develop surface films whose chemical composition is similar to that of the surface films developed on Li and lithiated carbon electrodes. In situ FTIR, EIS, AFM and EQCM revealed that at an onset around 1.5 V vs. Li/Li^+, alkyl carbonates, esters and salt anions such as AsF_6^-, PF_6^-, $CF_3SO_3^-$, $NS(O_2CF_3)_2^-$ and $C(SO_2CF_3)_3^-$ are reduced and insoluble organic and inorganic Li salts are precipitated on the electrodes' surfaces. Ethers are reduced at potentials below 0.5 V (Li/Li^+). The surface species thus formed are not stable and partially dissolve until their concentration in solution reaches saturation. In general, it can be said that during the cathodic processes of non-active electrodes in the commonly used Li salt solutions within the potential range of 2–0 V (Li/Li^+), about two thirds of the charge involved is injected into the solutions. Only one third of the charge is related to the formation of steady surface species. Thus, it appears that although all the reduction products of commonly used solvents and salts are insoluble Li salts, their precipitation on the solid electrodes as surface films is not immediate. The mechanism of the surface film formation in these cases involves several steps: charge injection into solution species, formation of reduction products in the vicinity of the electrode surface, precipitation of surface films and their partial dissolution, and reprecipitation of surface species of the lowest solubility product. It should be emphasized that this scenario is also relevant to carbon electrodes as well. Carbon anodes are usually introduced into solutions (in both laboratory experiments and practical batteries) in their

A strategy for R&D of Li and Li ion Batteries.

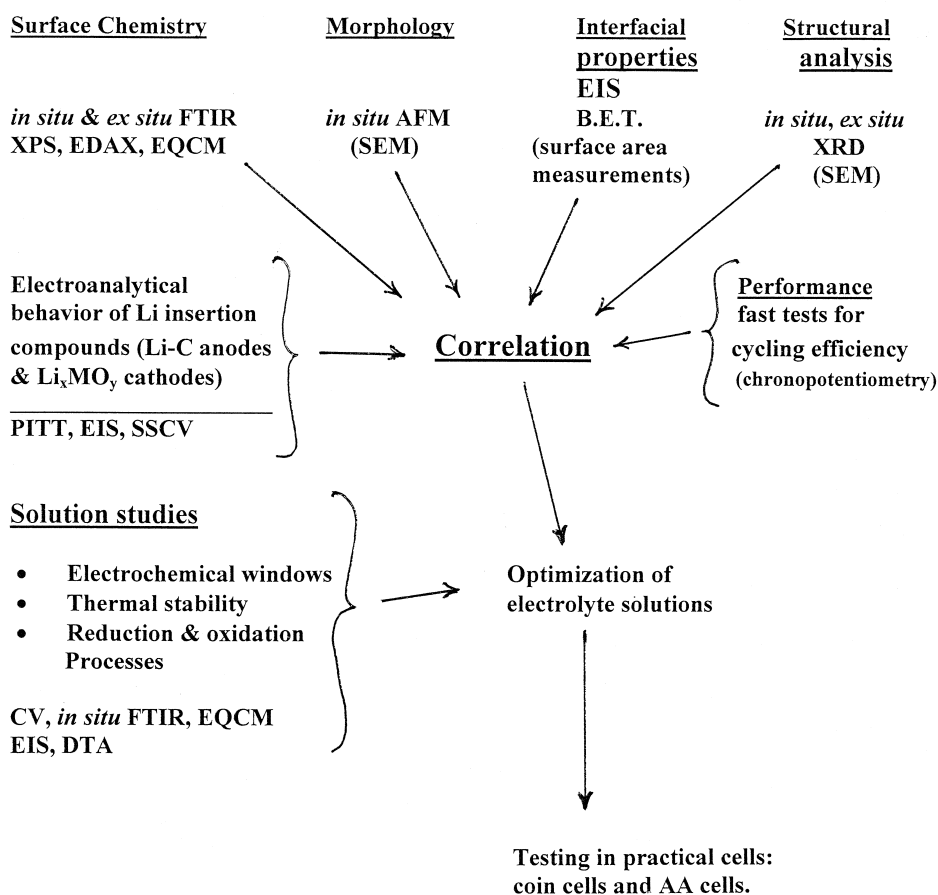## Study of Electrodes
Li, Li-C anodes and Li$_x$MO$_y$ cathodes.

Surface Chemistry

in situ & *ex situ* FTIR
XPS, EDAX, EQCM

Morphology

in situ AFM
(SEM)

Interfacial properties
EIS
B.E.T.
(surface area measurements)

Structural analysis

in situ, *ex situ*
XRD
(SEM)

Electroanalytical behavior of Li insertion compounds (Li-C anodes & Li$_x$MO$_y$ cathodes)

PITT, EIS, SSCV

Correlation

Performance
fast tests for cycling efficiency
(chronopotentiometry)

Solution studies

- Electrochemical windows
- Thermal stability
- Reduction & oxidation Processes

CV, *in situ* FTIR, EQCM
EIS, DTA

Optimization of electrolyte solutions

Testing in practical cells:
coin cells and AA cells.

Fig. 1. A scheme of an appropriate strategy for research directed towards the development of Li and Li ion batteries.

pristine, delithiated form. The first process is usually galvanostatic charging which lithiates the carbon. The carbons are thus gradually polarized to low potentials, allowing solvent and salt anion reduction to occur as the potential reaches the relevant onset values. Thus, the surface films on carbon electrodes are formed in a gradual process in which the most reactive solution components are reduced first.

In the case of Li electrodes, when fresh Li is exposed to solution, reduction processes of all solution components take place at low selectivity. However, as surface species precipitate on the active surface, they block it, and thus further reduction of solution species occurs at higher selectivity. Because of this, the surface films formed on lithium have a multilayer structure. This is illustrated in Fig. 2. Finally, the surface films formed on lithium and lithiated carbon electrodes have both a multilayer and mosaic-type microstructure, due to the variety of surface reactions that may take place. These include: various reduction processes

of solution components; secondary reactions of surface species with solution components; hydration of surface species; water diffusion through the film and water reduction; dissolution of surface species and redeposition of surface species whose concentration in solution reached saturation point.

These situations may induce highly non-uniform current distribution in Li dissolution–deposition processes. This is well reflected in morphological studies of Li electrodes in the various Li–salt solutions. Fig. 3 presents AFM images of Li electrodes obtained in situ in a variety of electrolyte solutions after Li deposition, as indicated. The images of Fig. 3 demonstrate that the morphology of Li electrodes is different in each electrolyte solution. This is due to the mosaic-type microstructure of the surface films, which differs from solution to solution (due to the unique surface chemistry developed in each electrolyte solution). The surface chemistry developed on Li and lithiated carbon electrodes was extensively studied, as already reported
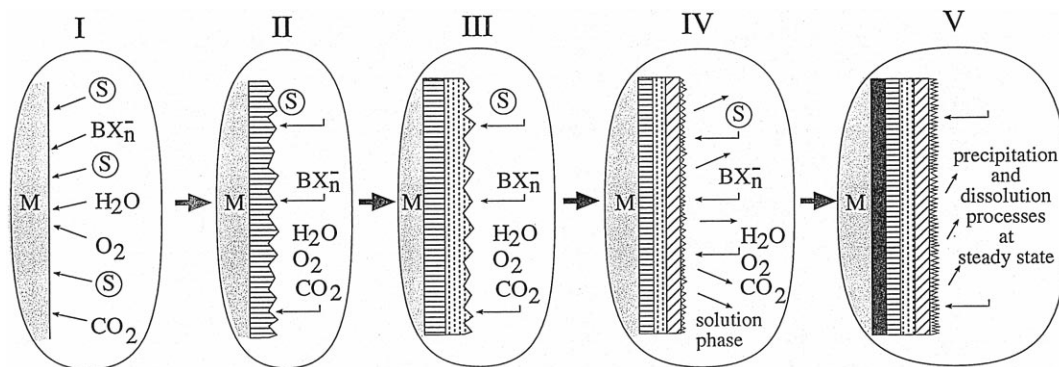
Fig. 2. A schematic illustration describing the formation of surface films on active electrodes.

[3,4,7,9,10]. A few important aspects related to recent studies are reviewed below.

3.2. Report on a few new important insights into the surface chemistry of Li and Li–C electrodes

There are only a few electrolyte solutions in which Li metal anodes are sufficiently reversible for secondary battery application. There are reports on EC-2Me-THF/LiAsF$_6$ solutions [12,13], 2Me-THF/THF/2Me-furane/LiAsF$_6$ mixtures [14], and 1–3 dioxolane/LiAsF$_6$ solutions stabilized with tributylamine (TBA) [1]. In fact, these three combinations are the only liquid systems that seem relevant to secondary Li batteries with metal anodes. It should be emphasized that solutions comprising salts other than LiAsF$_6$ are not suitable for long cycle life, Li metal secondary batteries.

Based on our extensive studies, the following conclusions could be drawn.

(1) LiAsF$_6$ is important because it is reduced on Li to form LiF and Li$_x$AsF$_y$ compounds. The presence of arsenic compounds on the Li surface modifies its reactivity and leads to uniform Li deposition–dissolution processes. It can be said that the Li metal is doped by arsenic, which reduces its reactivity.

(2) 2Me–furane, which was found to be an important additive, serves mostly as a Lewis acid trace scavenger. The source of the Lewis acids is usually the oxidation reaction of solution components taking place on the cathode side. The presence of 2Me–furane prevents polymerization of the ether solvents by trace Lewis acids.

(3) In the case of 1–3 dioxolane, the surface chemistry is complicated. Surface films comprised of HCOOLi (Li formate), CH$_3$CH$_2$OCH$_2$OLi and/or LiCH$_2$CH$_2$-OCH$_2$OLi and oligomers of poly DN with OLi edge groups (in addition to the above AsF$_6^-$ reduction products)

are formed. We believe that the presence of oligomeric species on the surface, making the surface films elastic, is of special importance. These elastic components suppress dendrite formation and enable Li deposition to occur beneath the surface films that remain protective and passivating for the newly formed Li deposits.

(4) In general, alkyl carbonate solvents, as well as their mixtures with ethers, are very problematic for use in secondary batteries with Li metal anodes. These solvents are reactive with lithium, and the surface chemistry is too complicated to provide uniform, highly protective surface films. One would expect the basic reaction of alkyl carbonates on Li surfaces to be:

$$R'OCO_2R'' + 2e^- + 2Li^+ \rightarrow Li_2CO_3 + R'R''.$$
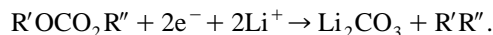
R'R'' = alkene for cyclic molecules (e.g., EC, PC) or alkane for opened chain molecules (DMC, DEC, EMC, etc.).

However, we found that the major products of the reactions of all the relevant alkyl carbonate solvents are ROCO$_2$Li species. In the case of opened chain molecules, ROLi surface species are also formed. Most of the ROCO$_2$Li species are not sufficiently good passivating agents for Li surfaces. An exception may be the (CH$_2$OCO$_2$Li)$_2$, which is the EC reduction product. This species is the best protective agent for Li surfaces of all the other ROCO$_2$Li or ROLi species formed on Li electrodes in alkyl carbonate solvents.

It appears from in situ FTIR spectroscopic studies that the expected product, Li$_2$CO$_3$, is not formed initially when fresh Li is exposed to alkyl carbonate solvents [15]. Li$_2$CO$_3$ becomes an important surface species only upon the aging of Li electrodes in solutions by in two parallel ways.
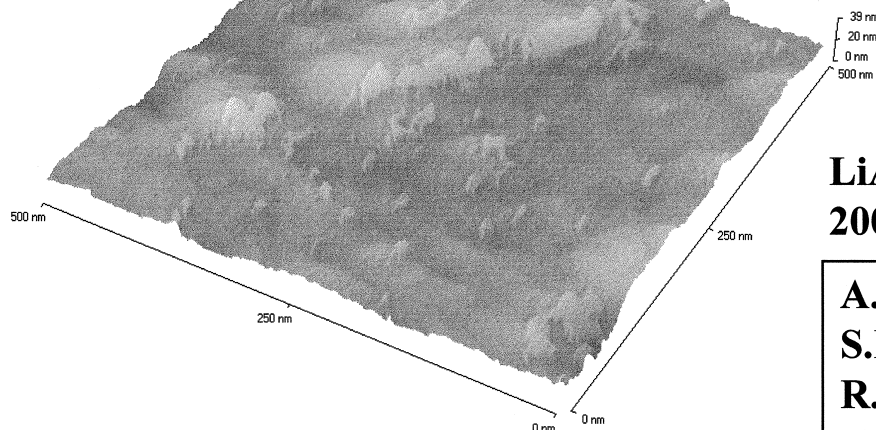
(1) The ROCO$_2$Li molecules formed initially react with trace water:

$$2ROCO_2Li + H_2O \rightarrow Li_2CO_3 + 2ROH + CO_2.$$

**Scan Area:
500nm × 500nm**

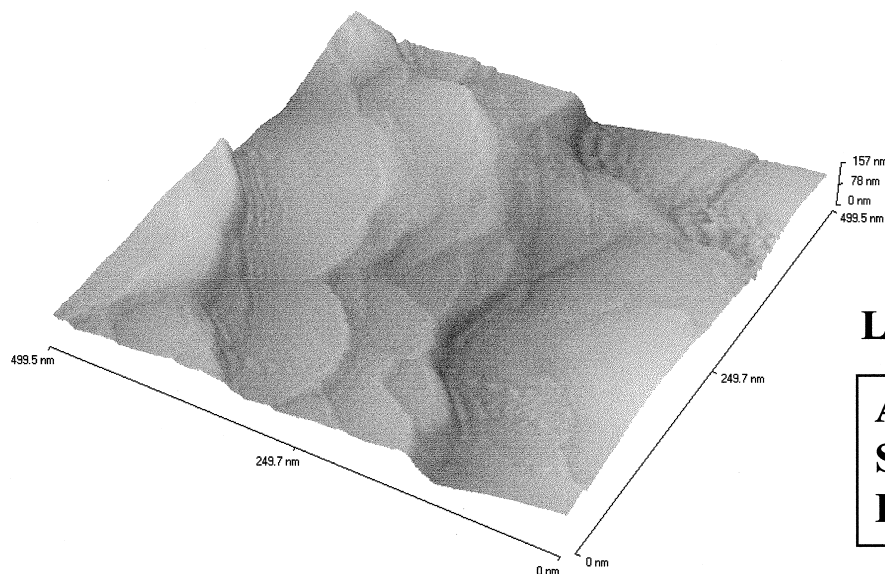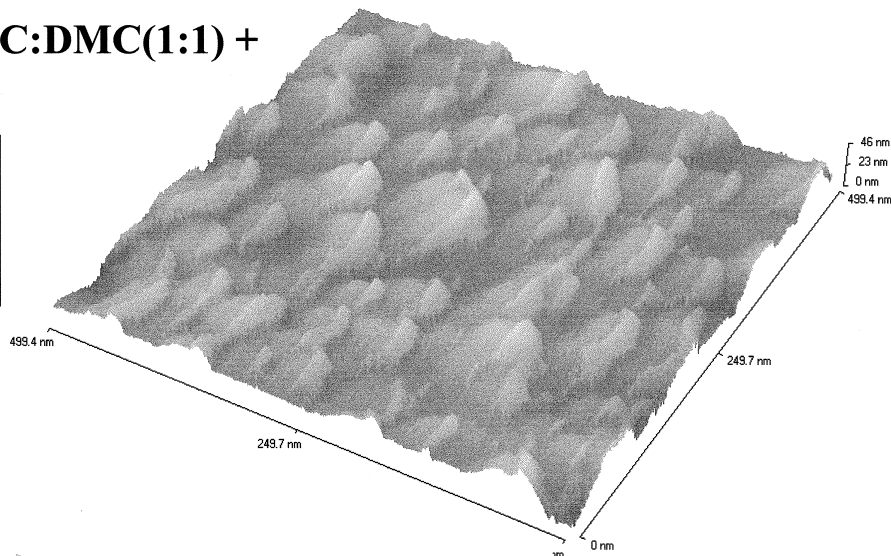# Deposition 0.4 C/cm²

**LiAsF$_6$ (0.5M) / PC +
200ppm water**

> **A.H. = 16.56 nm
> S.D. = 3.80 nm
> R.F. = 1.499**

**LiAsF$_6$ (0.5M) / EC:DMC(1:1) +
200ppm water**
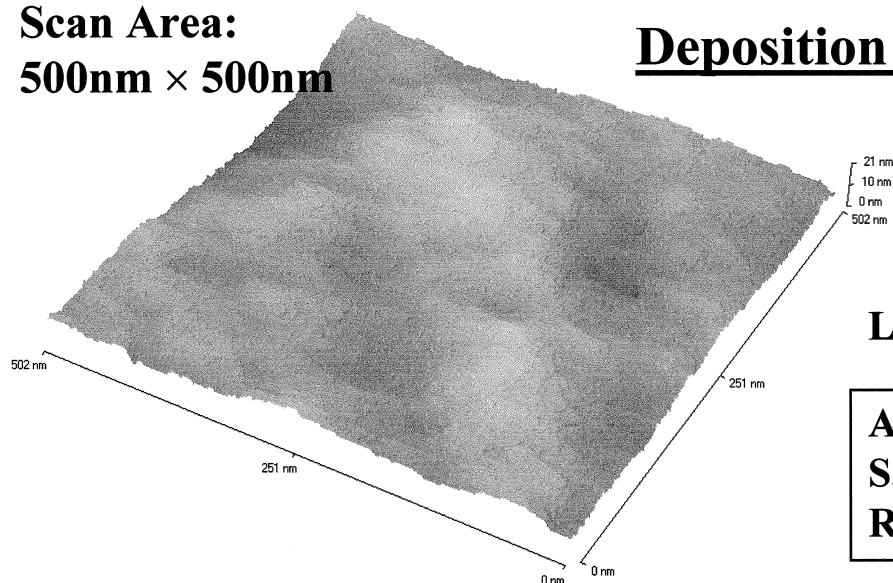
> **A.H. = 21.13 nm
> S.D. = 5.58 nm
> R.F. = 1.813**

LiAsF$_6$ (0.5M) / PC

> **A.H. = 82.84 nm
> S.D. = 20.13 nm
> R.F. = 2.117**

Scan Area:
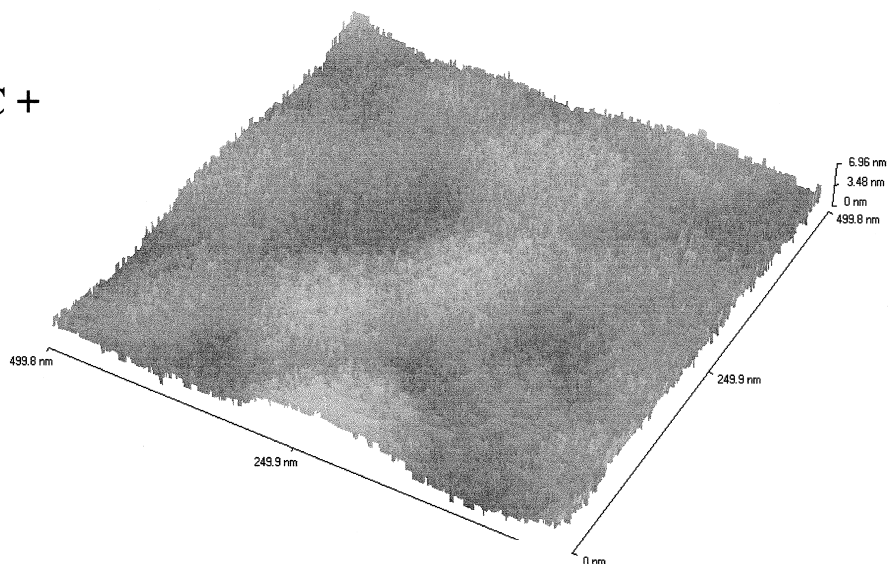**500nm × 500nm**

Deposition 0.4 C/cm²

21 nm
10 nm
0 nm
502 nm

251 nm

502 nm

251 nm

0 nm   0 nm

LiPF$_6$ (0.5M) / PC

A.H. = 11.29 nm
S.D. = 2.28 nm
R.F. = 1.422

LiPF$_6$ (0.5M) / PC +
200 ppm water

A.H. = 2.98 nm
S.D. = 0.86 nm
R.F. = 1.506

6.96 nm
3.48 nm
0 nm
499.8 nm

249.9 nm

499.8 nm

249.9 nm

0 nm

30 nm
15 nm
0 nm
502 nm

502 nm

251 nm

251 nm

0 nm   0 nm
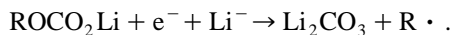
LiAsF$_6$ (0.5M) / PC +
Alumina

A.H. = 13.58 nm
S.D. = 2.86 nm
R.F. = 1.541
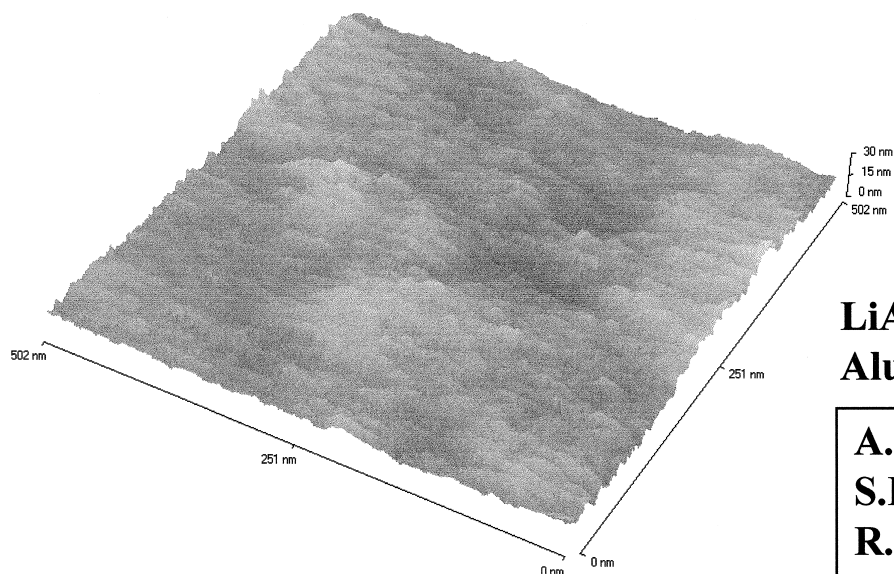
(2) Further reduction of $ROCO_2Li$ during aging.

$$ROCO_2Li + e^- + Li^- \rightarrow Li_2CO_3 + R \cdot .$$

Li_2CO_3 is also formed on Li surfaces in mixtures of PC or EC with ethers or opened chain alkyl carbonates in which the EC or PC concentration is low. From our studies it appears that EC or PC *can* undergo 2 electron reduction processes:

$$EC(PC) + 2e^- \rightarrow CO_3^= + alkylene(gas).$$

The carbonate thus formed is nucleophilic and reacts readily with EC or PC molecules:

$$CO_3^- + PC \rightarrow CH_3CH(OCO_2^-)CH_2OCO_2^-$$

$$CO_3^- + EC \rightarrow (CH_2OCO_2^-)_2.$$
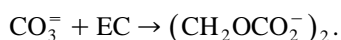
These organic carbonates react further with Li^+ ions and precipitate as surface species. However, at low EC or PC concentration the possibility of a nucleophilic reaction between $CO_3^=$ and EC or PC is not feasible. Thus, $CO_3^=$ reacts predominantly with Li^+ ions and Li_2CO_3 becomes a major surface species.

It should be emphasized that Li_2CO_3 is one of the best passivating agents for Li or Li–C electrodes. Surface films comprised of Li_2CO_3 as a major component are thin, compact, and lead to low interfacial impedance of Li or Li–C electrodes. It is possible to extend Li_2CO_3 formation on Li surfaces in solutions by the use of CO_2 as an additive [16]. It is important to comment that 'native' lithium metal is covered by surface films which also comprise Li_2CO_3. However, in addition to Li_2CO_3, these native films also contain Li_2O, Li_3N and LiOH, resulting from reactions of the active metal with the various atmospheric components. Due to this variety of components, the 'native' surface film that covers pristine Li electrodes does not have good passivating properties, although it contains Li_2CO_3. Its multicomponent structure induces non-uniform Li deposition and dissolution in most of the relevant electrolyte solutions used in secondary Li batteries. The fact that Li electrodes in EC or PC solutions are much better passivated and behave more reversibly in the presence of CO_2 (because of Li_2CO_3 formation) is further proof that Li_2CO_3 is *not* a major surface species on Li electrodes in EC or PC solutions. There is still an unanswered question as to whether the surface films formed on Li or Li–C in EC or PC are also comprised of polymeric species. There are reports that polycarbonate film is formed on lithiated graphite in EC solutions [17]. It should be emphasized that it is very difficult to find clear spectroscopic evidence for such a possibility because the absorption in the IR, UV–Vis and X-ray of polycarbonate species may be very similar to that of the parent alkyl carbonates.

Li or Li–C electrodes measured ex situ may always contain trace solvent molecules trapped in the surface films, and which should mask absorption of polycarbonate species, if present. It should be stressed that alkyl carbonate solvents *are not* suitable for use in secondary battery systems with Li metal anodes. These solvents are too reactive, the Li surface chemistry is very heterogeneous, and thus may induce highly non-uniform Li deposition–dissolution processes. Fig. 4 shows the results of charge–discharge cycling of Li electrodes (on Ni substrates) in
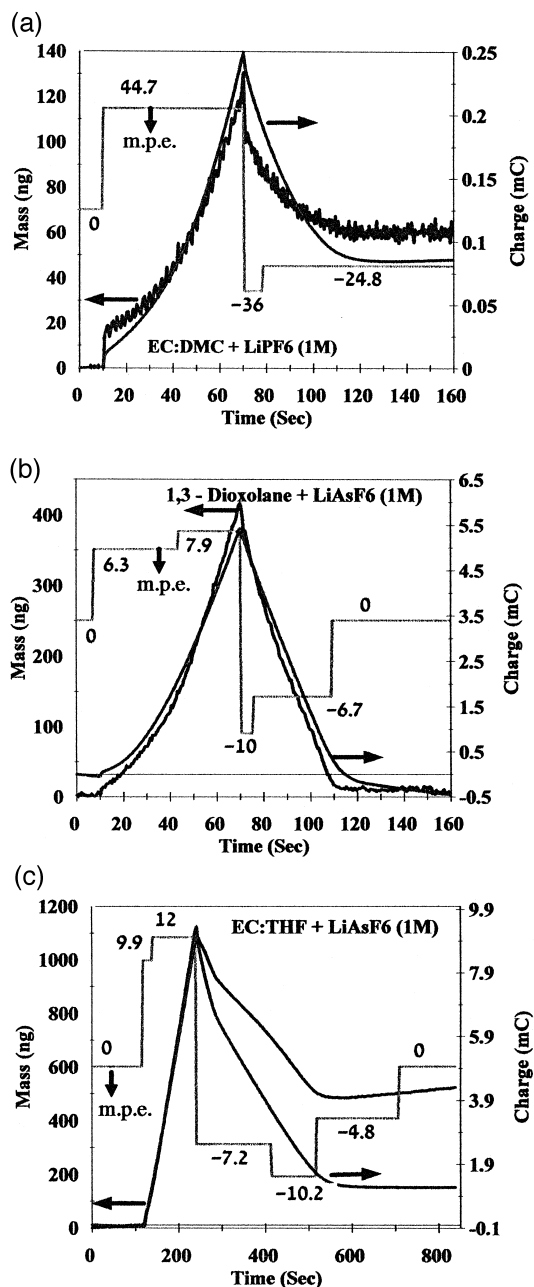

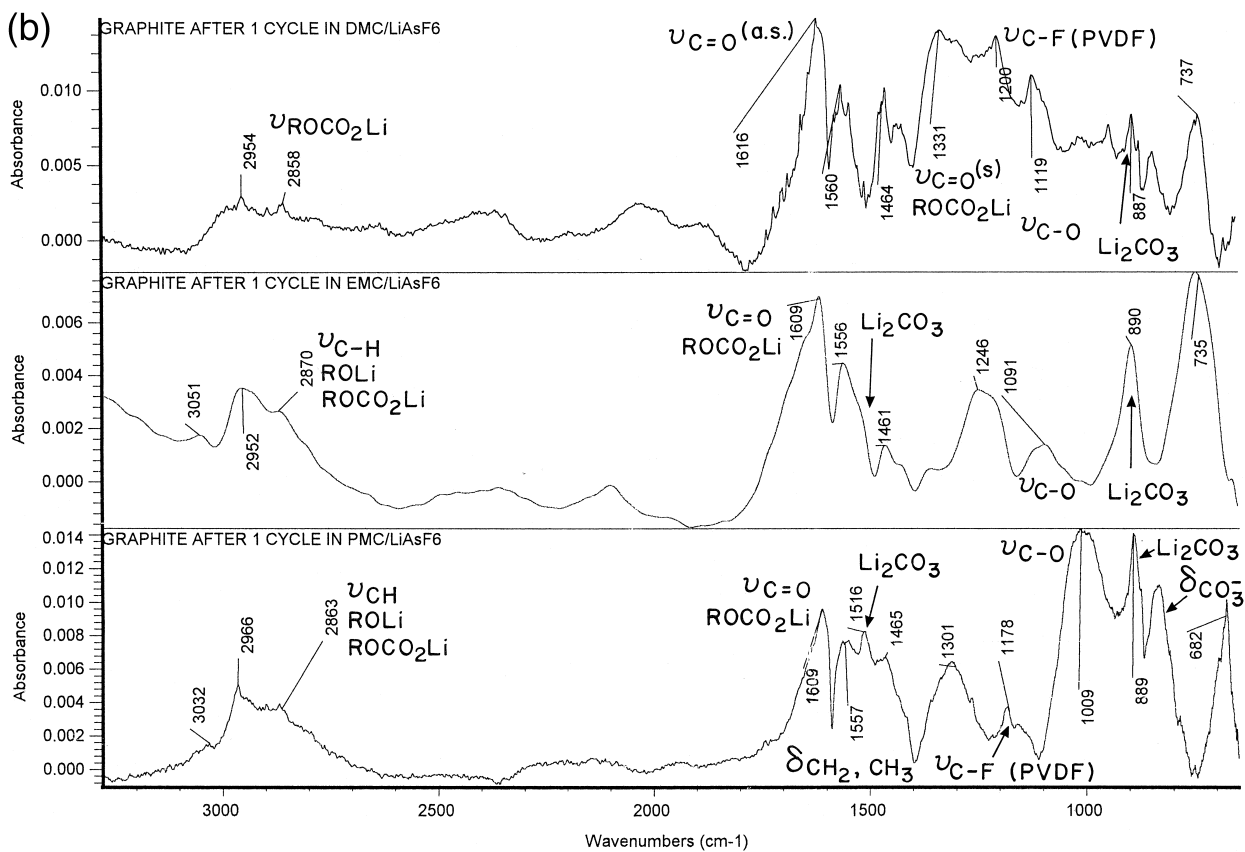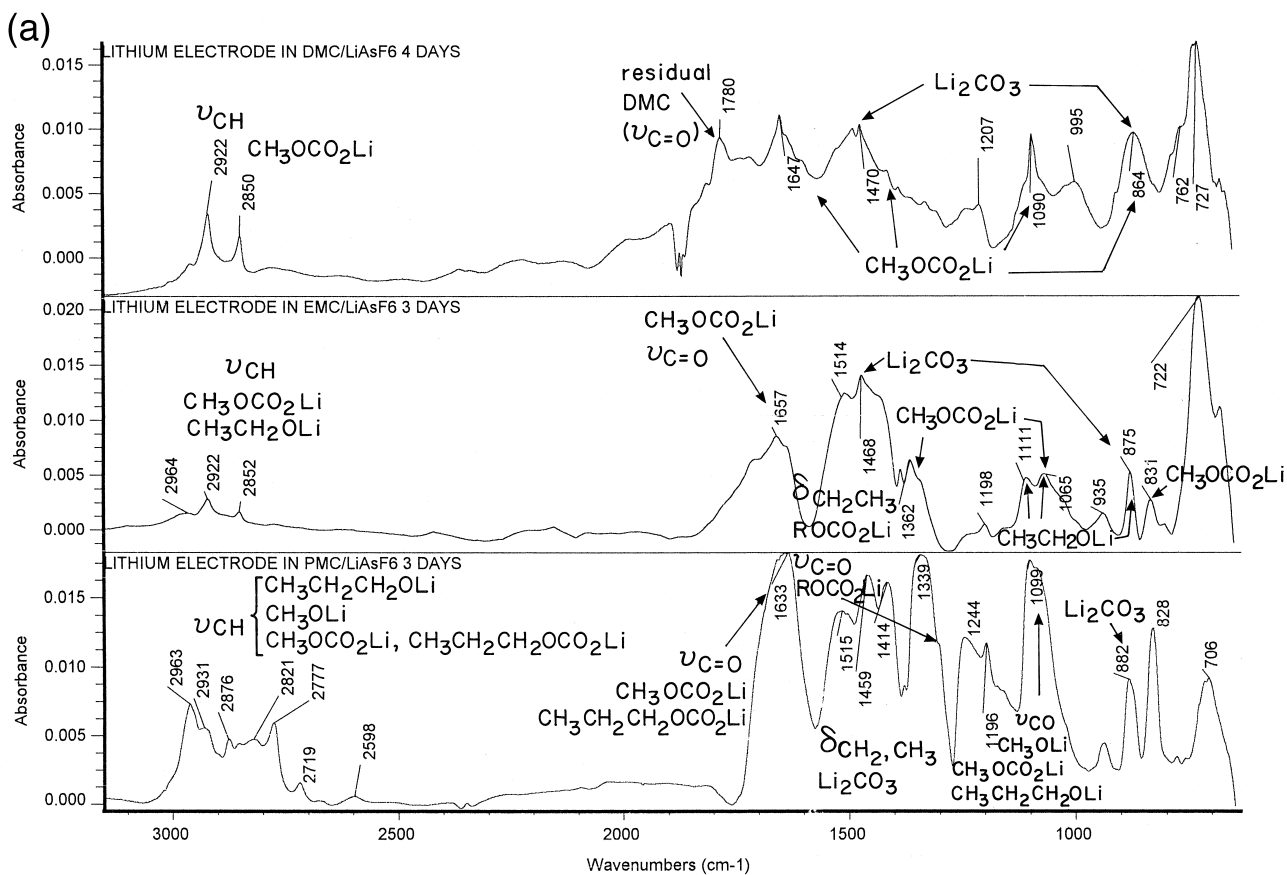Fig. 4. Typical results of EQCM experiments with Li electrodes on nickel substrates. The mass accumulation, the charge involved and the mass per mole of electrons calculated during a typical potentiostatic charge–discharge cycle are shown ($\pm$100 mV vs. Li/Li^+). (a) EC-DMC/$LiPF_6$ 1 M solution. (b) EC-THF/$LiAsF_6$ 1M solution. (c) 1–3 Dioxolane/$LiAsF_6$ 1M solution (stabilized with 1000 ppm of tributyl amine).

(a) Top panel: LITHIUM ELECTRODE IN DMC/LiAsF6 4 DAYS — υ_{CH}, CH_3OCO_2Li, peaks labelled 2922, 2850; residual DMC ($\upsilon_{C=O}$) 1780; 1647; Li_2CO_3 1470, 1207, 995, 864, 762, 727; CH_3OCO_2Li 1090.

Middle panel: LITHIUM ELECTRODE IN EMC/LiAsF6 3 DAYS — υ_{CH}, CH_3OCO_2Li, CH_3CH_2OLi, peaks 2964, 2922, 2852; CH_3OCO_2Li $\upsilon_{C=O}$ 1657; 1514; Li_2CO_3; CH_3OCO_2Li 1468, 1111, 875; 1362, 1198, 1065, 935, 831; δCH_2CH_3 $ROCO_2Li$; CH_3CH_2OLi; 722.

Bottom panel: LITHIUM ELECTRODE IN PMC/LiAsF6 3 DAYS — υ_{CH} { $CH_3CH_2CH_2OLi$, CH_3OLi, CH_3OCO_2Li, $CH_3CH_2CH_2OCO_2Li$ }, peaks 2963, 2931, 2876, 2821, 2777, 2719, 2598; $\upsilon_{C=O}$ $ROCO_2Li$ 1633, 1339; $\upsilon_{C=O}$ CH_3OCO_2Li $CH_3CH_2CH_2OCO_2Li$; 1515, 1459, 1414; $\delta CH_2, CH_3$ Li_2CO_3; 1244; 1196; υ_{CO} CH_3OLi CH_3OCO_2Li $CH_3CH_2CH_2OLi$ 1099; Li_2CO_3 882, 828; 706.

Wavenumbers (cm-1)

(b) Top panel: GRAPHITE AFTER 1 CYCLE IN DMC/LiAsF6 — υ_{ROCO_2Li} 2954, 2858; $\upsilon_{C=O}$ (a.s.) 1616; υ_{C-F} (PVDF) 1200; 1560, 1464, 1331; $\upsilon_{C=O}$ (s) $ROCO_2Li$; υ_{C-O} 1119; Li_2CO_3 887; 737.

Middle panel: GRAPHITE AFTER 1 CYCLE IN EMC/LiAsF6 — υ_{C-H} ROLi $ROCO_2Li$ 3051, 2952, 2870; $\upsilon_{C=O}$ $ROCO_2Li$ 1609; Li_2CO_3 1556, 1461; 1246, 1091; υ_{C-O} Li_2CO_3; 890, 735.

Bottom panel: GRAPHITE AFTER 1 CYCLE IN PMC/LiAsF6 — υ_{CH} ROLi $ROCO_2Li$ 3032, 2966, 2863; $\upsilon_{C=O}$ $ROCO_2Li$ 1609; Li_2CO_3 1516, 1465; υ_{C-O}; Li_2CO_3; δCO_3^-; 1557, 1301, 1178, 1009, 889, 682; $\delta CH_2, CH_3$; υ_{C-F} (PVDF).
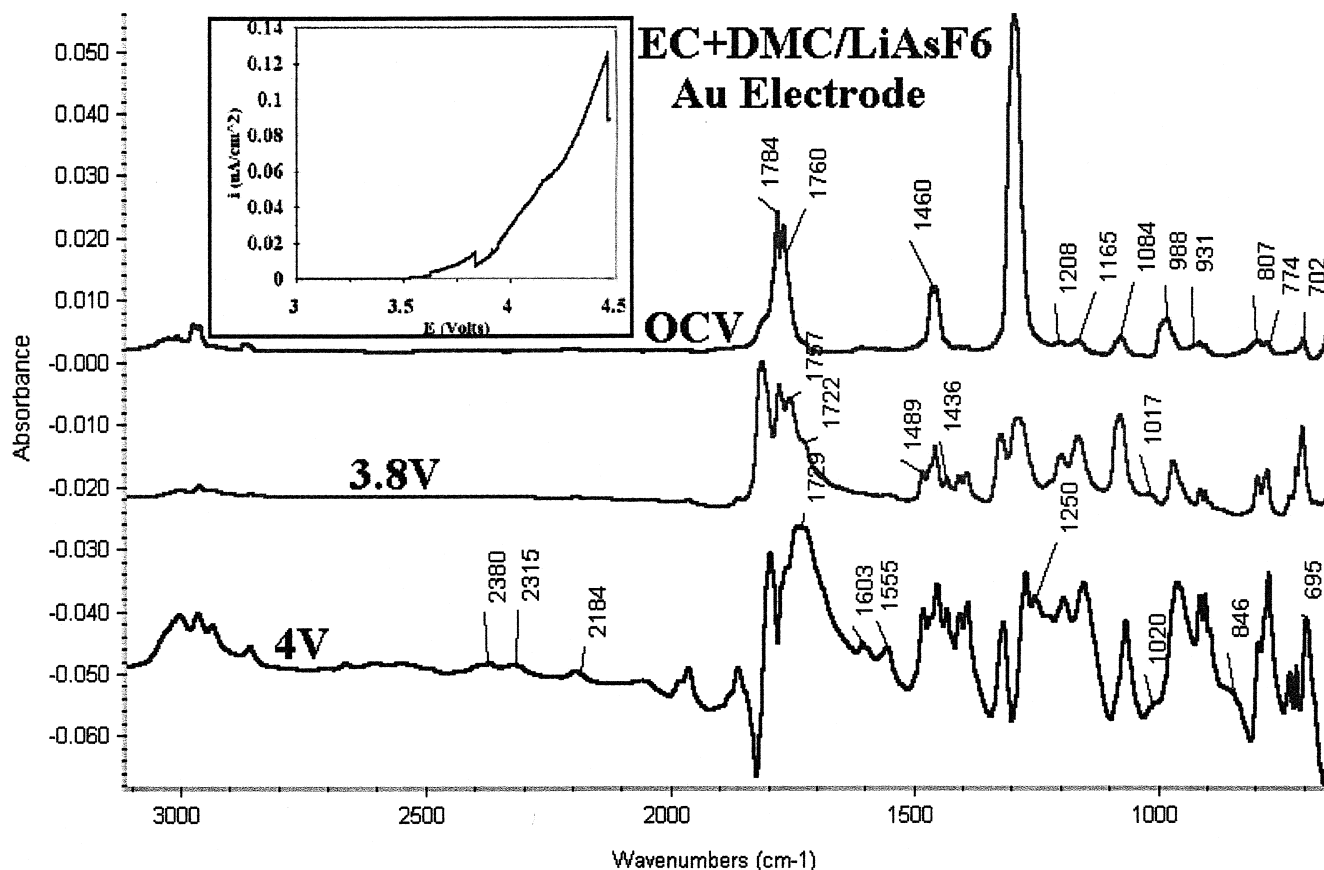
Wavenumbers (cm-1)

Fig. 6. FTIR spectra obtained in situ (single internal reflectance mode: SIR [3]), from Au electrodes at 3.8 and 4 V vs. Li/Li$^+$ (as indicated) in EC-DMC/LiAsF$_6$ solution. The potential was scanned anodically at 5 mV/s from OCV ($\approx$ 3 V vs. Li/Li$^+$), as shown in the voltammogram added in the upper left corner. The potential scanning was stopped for the measurements at fixed potentials. The spectra displayed were obtained by subtraction of the OCV spectrum shown (top).

LiAsF$_6$ solutions of DN, EC-DMC 1:1 and EC-THF 1:1 measured by electrochemical quartz crystal microbalance. The mass accumulation and depletion, the charge involved in a typical potentiostatic charge-discharge cycle (± 100 mV vs. Li/Li$^+$), and the calculated mass per mole of electrons (m.p.e.) are presented in this figure. These results demonstrate the superiority of DN solutions for use in Li metal, anode-based secondary batteries. However, it is possible to use alkyl carbonate solvents such as EC and PC in Li metal-based secondary batteries containing gel electrolyte. (The solvents are contained in a polymeric matrix). The use of gel electrolytes in secondary batteries may considerably improve the reversibility of Li metal anodes because of the pressure and surface tension applied to the Li electrodes in them (compared with liquid electrolyte solutions) [18].

When the anodes are lithiated carbons, alkyl carbonate solvents are very suitable because the electrochemical window is wide, and thus suitable for use with 4 V cathodes (in Li ion battery systems). In addition, the surface area of Li–C electrodes does not change considerably during charge–discharge cycling, as it does when Li metal anodes are used. It should be emphasized that the role of the passivation needed for Li–C anodes is quite different from that required for Li metal anodes. In the latter case, a good anode is obtained if the surface films prevent dendrite formation. This requires a highly uniform structure of the surface films, as well as a large degree of flexibility. In the case of Li–C anodes, the surface films have to be formed prior to the Li insertion process. They have to be sufficiently compact to prevent any diffusion of solution species through them, and to allow facile Li$^+$ ion

Fig. 5. (a) FTIR spectra measured ex situ (external reflectance mode) from Li electrodes (protected with KBr windows) which were freshly prepared in LiAsF$_6$ solutions of DMC, EMC and PMC, as indicated, and stored in solutions for a few days. Some peak assignments are also presented. (b) FTIR spectra measured ex situ (diffuse reflectance mode) from graphite electrodes after one completed intercalation–deintercalation cycle in LiAsF$_6$ solutions of DMC, EMC and PMC, as indicated.

Table 1
Onset potentials of oxidation for various alkyl carbonate solutions

Solution	Salt	Oxidation potentials V vs. Li/Li$^+$
EC:DEC 9:1	LiAsF$_6$	3.8
EC:DEC 1:1	LiAsF$_6$	3.9, 4.4
EC:DEC 1.9	LiAsF$_6$	4.2
EC:DMC 1:1	LiAsF$_6$	3.55, 3.75
DMC	LiAsF$_6$	3.8, 3.9
EC:DEC 1:1	LiClO$_4$	3.7, 4
EC:DEC 1:1	LiPF$_6$	3.75
EC:DEC 1:1	LiN(SO$_2$CF$_3$)$_2$	3.9, 4.3
EC:DEC 1:1	LiC(SO$_2$CF$_3$)$_3$	3.9, 4

When two numbers appear, the first value relates to the onset of a small background oxidation current and the second one to a current rise at higher potentials.

migration from the solution to the active mass. Such requirements do not need high uniformity and flexibility of the surface films. Thus, surface films comprised of Li salts such as Li$_2$CO$_3$ (CH$_2$OCO$_2$Li)$_2$ or LiF can be good enough. Highly reversible behavior of Li-graphite anodes was obtained in some asymmetric, opened chain alkyl

carbonates such as ethyl–methyl and propyl–methyl carbonates (EMC, PMC) [19,20]. This is in contrast to the poor performance of Li–C anodes in symmetric alkyl carbonates such as DMC and DEC. The reason for this difference in behavior obviously relates to the surface chemistry developed on Li–C electrodes in these solutions.

We investigated the surface chemistry of lithiated graphite electrodes cycled in solutions of the above alkyl carbonates, and for that we used FTIR spectroscopy in diffuse reflectance mode. We should point out that such studies are difficult. However, studying the surface chemistry developed on lithium metal electrodes in these solutions as a prerequisite helps in understanding and interpreting the complicated FTIR spectra obtained from the powdered carbon electrodes. Fig. 5 compares FTIR spectra measured from Li and Li–graphite electrodes (Fig. 5a and b, respectively) treated in LiAsF$_6$ solutions of EMC, PMC and DMC. The spectra in Fig. 5a were obtained from Li electrodes freshly prepared in solutions, stored for a few days, and then measured ex situ. The spectra in Fig. 5b were obtained from graphite electrodes after one completed cycle of lithiation–delithiation. Major peak analysis
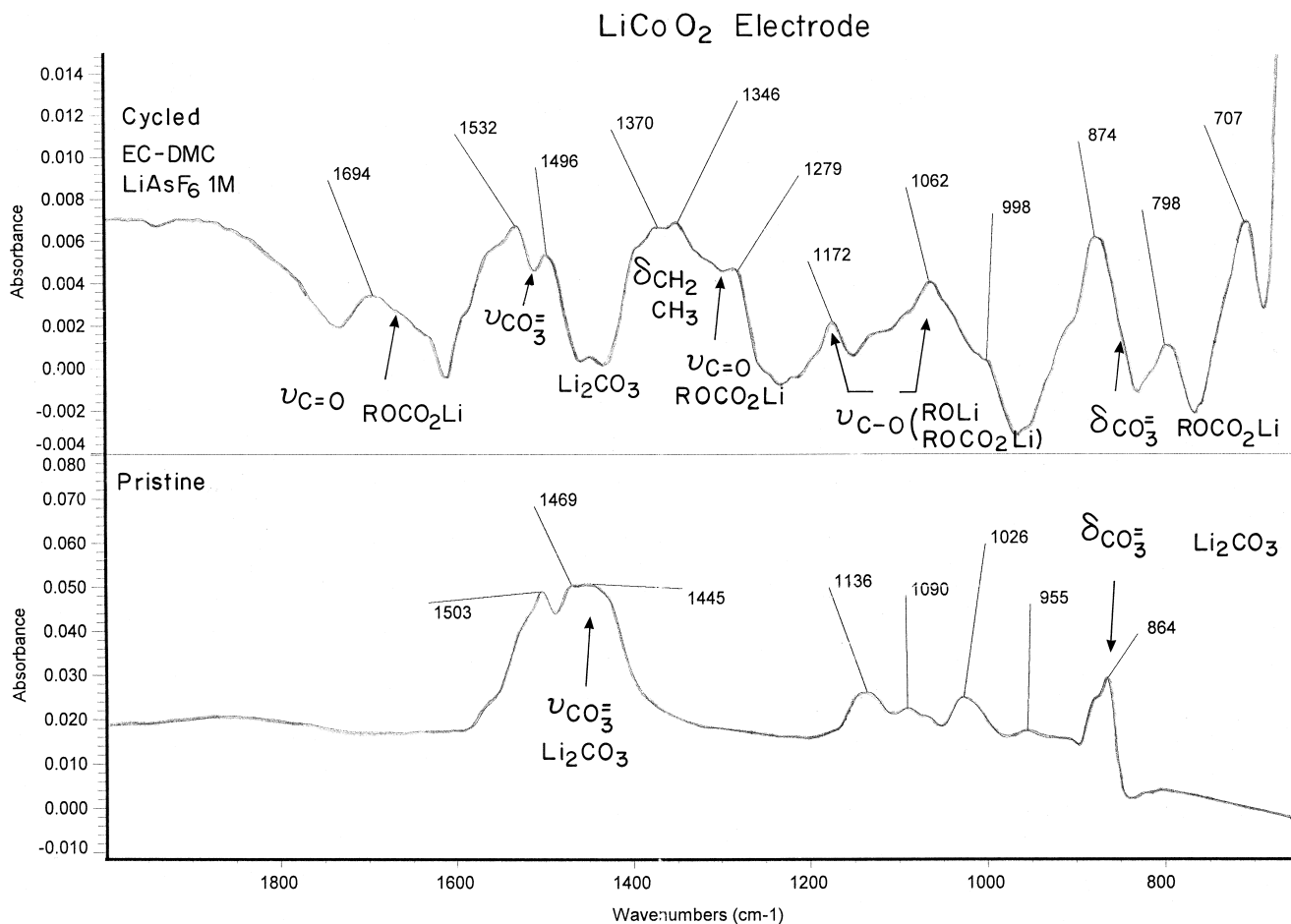

Fig. 7. FTIR spectra measured (diffuse reflectance mode) from a pristine LiCoO$_2$ electrode and a LiCoO$_2$ cycled (about 20 deintercalation–intercalation cycles, 3–4.2 V vs. Li/Li$^+$) in EC-DMC/LiAsF$_6$ solution. The counter electrode was lithium–metal. The spectra and some peak assignments are indicated.

appears in the spectra of both figures. it is clear that the spectra measured from the Li electrodes are of a high resolution and enable identification of the surface species formed.

In DMC, CH_3OCO_2Li is a major surface species, while some Li_2CO_3 and trace CH_3OLi are also formed. In EMC, CH_3OCO_2Li and Li_2CO_3 are the major surface species. Trace CH_3CH_2OLi, CH_3OLi and $CH_3CH_2OCO_2Li$ may also be formed. In PMC we identify all the four possible reduction products: CH_3OCO_2Li, $CH_3CH_2CH_2OCO_2Li$, CH_3OLi and $CH_3CH_2CH_2OLi$, and Li_2CO_3. The spectra measured from the graphite electrodes are of a worse resolution. However, due to their general similarity to the spectra measured with the Li electrodes, we assume that both types of electrodes develop similar surface chemistry in the same solutions. We attribute the good performance of Li–graphite electrodes in EMC and PMC solutions to a pronounced Li_2CO_3 precipitation on the electrode surface. The solvent reduction products are more soluble in EMC and PMC than in DMC.

Hence, after the initial precipitation of solvent reduction products on the graphite electrodes (which enables their passivation), their partial dissolution allows Li_2CO_3 (formed mostly by reactions between $ROCO_2Li$ and trace

water) to reprecipitate. This replacement enhances the electrode's passivation. In DMC, the solvent reduction products are less soluble and thus, they control the electrode's passivation, which is not as good as in the presence of Li_2CO_3 as a major surface species.

3.3. Oxidation of solutions and the surface chemistry of the cathodes

In most of the commonly used Li ion battery systems, the cathodes are polarized to potentials that may reach 4.5 V (Li/Li^+). Hence, the question of the anodic stability of electrolyte solutions for Li ion batteries is critical. It appears that the onset of oxidation of many alkyl carbonate-based solutions on noble metal electrodes occurs at potentials below 4 V (Li/Li^+). We usually observe low oxidation currents (in the order of $\mu A/cm^2$) starting at onset potentials between 3.5–3.9 V. The current rise related to an intense oxidation process is then observed at onset potentials usually above 3.9 V.

Table 1 summarizes information on the oxidation potentials of various commonly used electrolyte solutions with noble metal electrodes. A similar picture is obtained with electrodes such as aluminum.
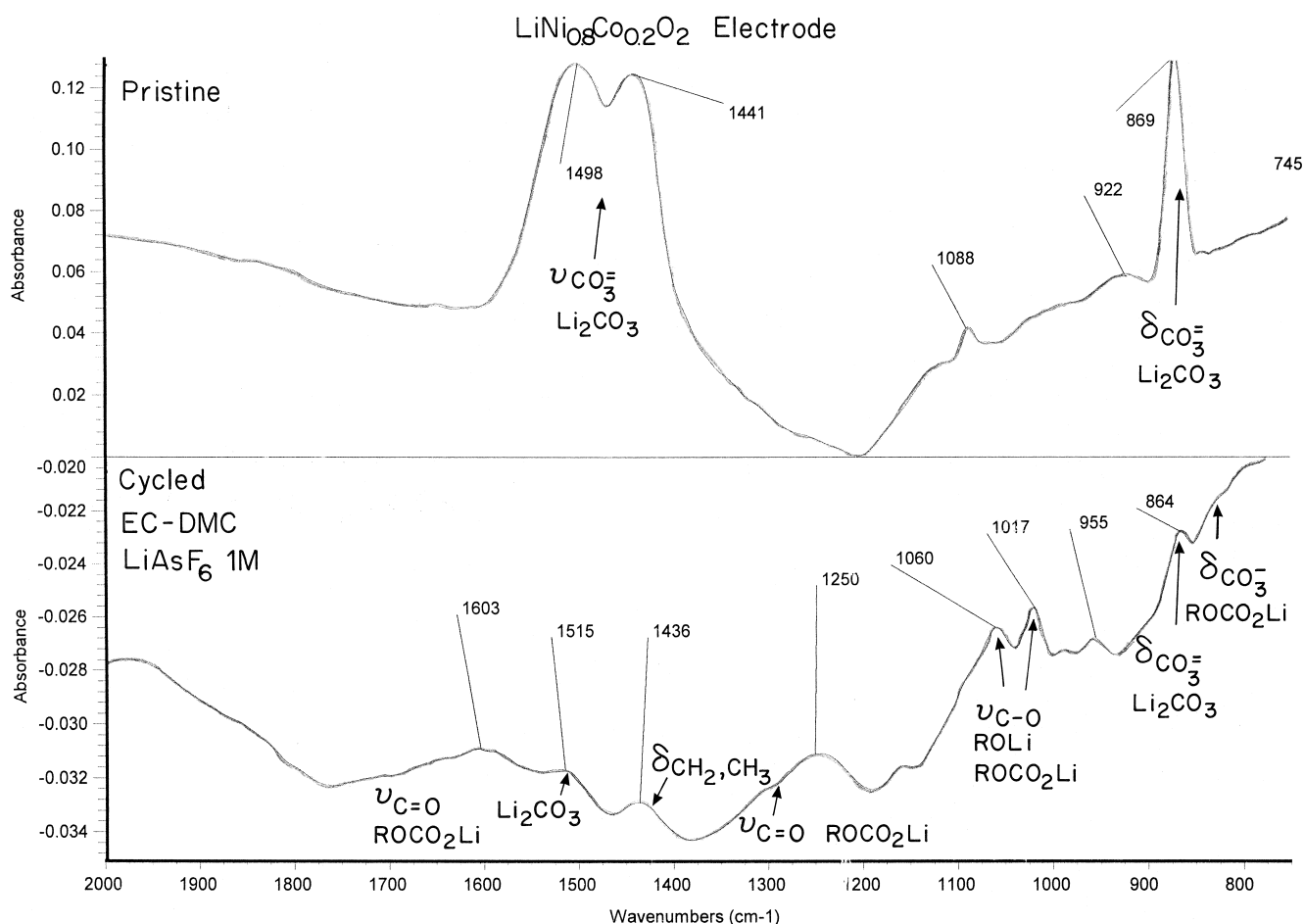

Fig. 8. $LiNi_{0.8}Co_{0.2}O_2$ electrode. (The electrode was treated and measured as in Fig. 7).

Fig. 6 shows FTIR spectra measured in situ during oxidation of EC-DMC/LiAsF$_6$ solution on an Au electrode. The voltammogram of the experiment is also shown in this figure in the upper left corner. The potential was scanned at 5 mV/s from OCV and the scanning was stopped at 3.8 and 4 V (Li/Li$^+$) for the spectral measurements at constant potentials (indicated). An OCV solution spectrum is also shown. The spectrum measured at 4 V is markedly different from the OCV spectrum. It shows a pronounced peak around 1730 cm^{-1} that may be attributed to an oxidation product of the alkyl carbonates whose carbonyl group is attached only to one oxygen group (as it is in esters). Very significant are the peaks around 2315–2380 and 2170 cm^{-1} that can be attributed to CO$_2$ and CO, respectively. Both moieties are expected products of alkyl carbonate decomposition. Further analysis of oxidation patterns for alkyl carbonates based on these spectral studies are beyond the scope of this paper.

It should be noted, however, that on the cathodes relevant to Li ion batteries, the oxidation processes of the solvents are much less pronounced than on noble metal electrodes. This is due to the fact that the cathodes are composite electrodes that include active mass with relatively low conductivity, and polymeric binder (e.g., PVDF)

which cover most of the active mass as a thin membrane. In addition, the active mass, which are usually Li$_x$MO$_y$ compounds (M = transition metal), is covered with surface films, as discussed below. The surface chemistry of the cathode materials is also an important issue that has to be properly addressed. We investigated the surface chemistry of a variety of cathode materials using FTIR spectroscopy.

Figs. 7 and 8 show FTIR spectra of pristine and cycled LiCoO$_2$ and LiNi$_{0.8}$Co$_{0.2}$O$_2$ electrodes, respectively, in EC-DMC/LiAsF$_6$ solutions. As shown in these figures, the spectra of the pristine active mass of both electrodes are typical of Li$_2$CO$_3$. This is true for Li$_x$Mn$_2$O$_4$ spinel electrodes as well. Upon cycling, the electrodes develop surface films whose spectra are somewhat similar to those of ROCO$_2$Li species that are the major reduction products of the solvent. This is further demonstrated in Fig. 9. Surface films can be formed either by some reaction of the solvent molecules with the cathode materials (e.g., nucleophilic attack by negatively charged oxygen) or oxidation and precipitation of the oxidized species as insoluble salts. Another possibility is that ROCO$_2$Li species are formed in the anode side (either Li or Li–C), saturate the solution and then reprecipitate on the cathode. We compared the spectra of cathodes after prolonged cycling in EC-
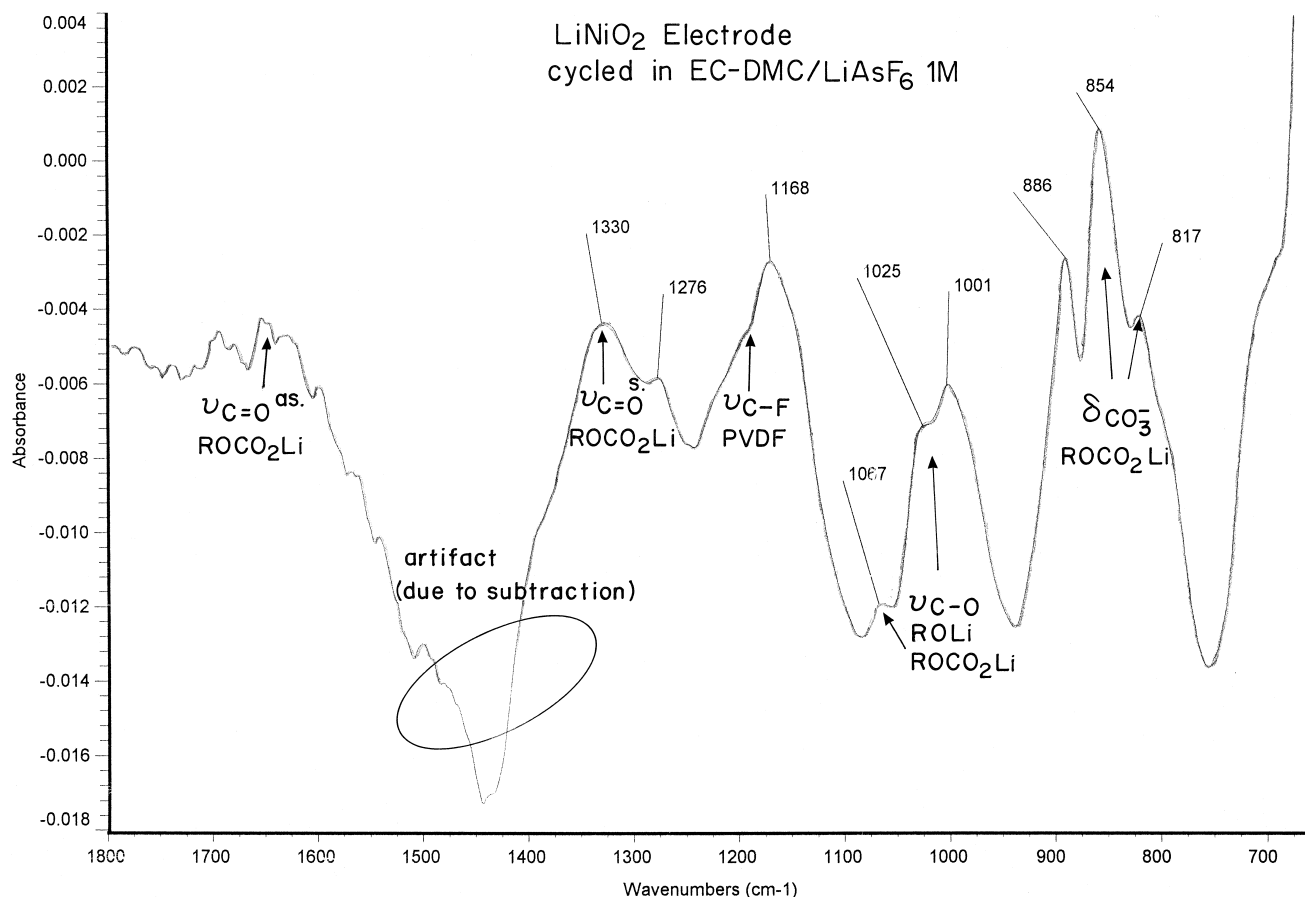

Fig. 9. FTIR spectrum measured (diffuse reflectance mode) from a LiNiO$_2$ electrode after 20 deintercalation–intercalation cycles (3–4.2 V vs. Li/Li$^+$) in EC-DMC/LiAsF$_6$ solution. The counter electrode was Li metal. Some peak assignments are presented in the figure.

DMC/LiAsF$_6$ solutions with spectra measured from electrodes polarized to high potentials (delithiation), and then stored in the same solution in the absence of anodes. We also compared them with spectra measured from electrodes stored in the presence of high surface area lithium (see Fig. 10). From these measurements it appears that one of the sources of the surface films developed on the cathodes upon cycling may be the species formed on the anode due to solvent reduction. Hence, an important conclusion of this section is that the cathodes are also covered by surface films, thus making Li ion migration through them a necessary stage in the overall electrode process. In addition, despite the fact that alkyl carbons may be oxidized on noble metals at potentials below 4 V, massive oxidation of these solvents on cathode materials such as Li$_x$Mn$_2$O$_4$, Li$_x$NiO$_2$ or Li$_x$CoO$_2$ does not occur due to passivation phenomena.

3.4. Impedance spectroscopy of Li insertion electrodes and intercalation mechanisms

In general, Li insertion electrodes, including lithiated graphite, LiNiO$_2$, LiCoO$_2$ and LiMn$_2$O$_4$ electrodes show several common electroanalytical features. This is clearly reflected in measurements such as slow scan rate cyclic voltammetry (SSCV), potentiostatic intermittent titration (PITT) and impedance spectroscopy (EIS). Below are some common denominators in the behavior of these electrodes [7,8,11].

(1) Li insertion is a multistage process which includes, for both Li–C and LiMO$_x$ electrodes, Li$^+$ migration through surface films, charge transfer through interfaces, solid state diffusion within the active mass, and finally, accumulation in the bulk (potential dependent capacitive behavior).

(2) The Li insertion is, in most cases, accompanied by phase transition. It is also expected that due to the size of the Li ion, attractive interactions exist among the intercalation sites. This leads to two important electrochemical features. The SSCV is characterized by sets of narrow peaks (i.e., narrower than what would be expected for regular adsorption-type processes) with intrinsic hysteresis (which depends on both the thermodynamics and the kinetics of these systems). In addition, the chemical diffusion coefficient depends on the potential (a non-monotonous function). It is minimal at the SSCV peak potentials.

(3) It should be emphasized that the diffusion length in these electrodes does not relate to their thickness, but rather to the size of the particles. The usual structure of these composite electrodes allows the binder to partially
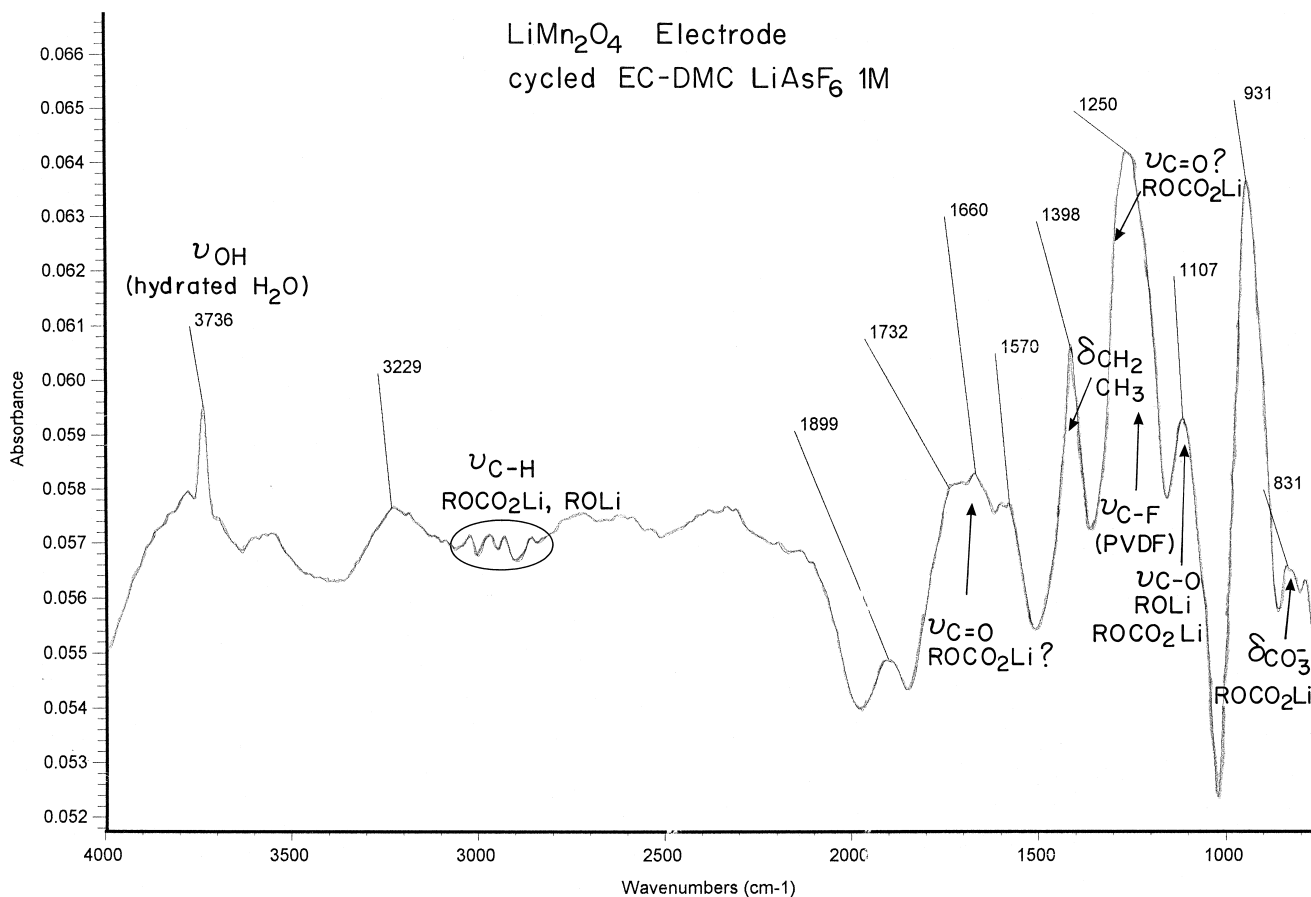

Fig. 10. FTIR spectrum measured (diffuse reflectance mode) from a LiMn$_2$O$_4$ electrode that was stored for 14 days in EC-DMC/LiAsF$_6$ solution containing lithium. (The solution was probably saturated with the products of solvent reduction by lithium).

swell the solution, and it then penetrates the electrode's pores. Thus, most of the particles react with the solution species (and, most important, with Li^+ ion) in parallel. Hence, Li^+ diffusion into the active mass starts at the envelope of facets perpendicular to the basal planes of layered materials such as graphite or $LiCoO_2$. The diffusion length may therefore by taken as half of the average particle size.

(4) EIS spectra measured from Li–graphite $LiNiO_2$, $LiCoO_2$ or $LiMn_2O_4$ electrodes at different intercalation stages clearly reflect the multistep nature of the overall Li insertion processes. In many cases, a good separation of the relevant time constants is obtained.

Fig. 11 presents four typical Nyquist plots obtained from the four above electrodes, as indicated. The base potentials of these measurements are marked. A general model for these spectra is also shown in Fig. 11, which includes all the time constants relevant to these electrodes, which are clearly reflected by the EIS spectra. The model includes a 'Voight'-type analog (several $R \| C$ circuits in series) which reflects Li^+ ion migration through surface films, charge transfer resistance coupled with double layer capacitance, a finite length Warburg-type element for solid state Li diffusion, and finally, the intercalation capacitance. Note that R_{CT} is potential dependent as well as C_{int}. (The peaks appearing in the SSCV reflect the potential dependence of the differential intercalation capacitance). We attribute R_{CT} and C_{DL} to the interface between the surface films and the active mass.

Impedance spectroscopy is an important tool for studying the capacity fading mechanism of these electrodes because it enables one to distinguish between cases in which the capacity decreases due to structural changes in the active mass, and cases in which the capacity fading in due to a slow-down of the electrodes' kinetics (due to interfacial phenomena). We demonstrate the use of impedance spectroscopy for studying the behavior of Li insertion electrodes, as applied to lithiated graphite electrodes during prolonged cycling.

Fig. 12 compares impedance spectra measured with a graphite electrode comprised of particles of 25 μm average size and PVDF binder (10% by weight) at different potentials during intercalation, after 3 cycles in EC-DMC/$LiAsF_6$ solution. Fig. 13 compares impedance spectra measured with a similar electrode in the same solution (as per Fig. 11) at 110 mV (vs. Li/Li^+) during intercalation, after different cycles. Fig. 14 compares impedance spectra measured from two types of graphite electrodes (25 and 44 μm average particle size) at different potentials, and other different cycles as indicated.

Some conclusions drawn from these spectra and the related measurements are summarized below.

(1) The impedance spectra clearly reflect four major sets of time constants: (a) A high frequency, flat semicircle that can be modeled by a 'Voight'-type analog of 3–5 $R \| C$ circuits in series. (b) Another low frequency, flat
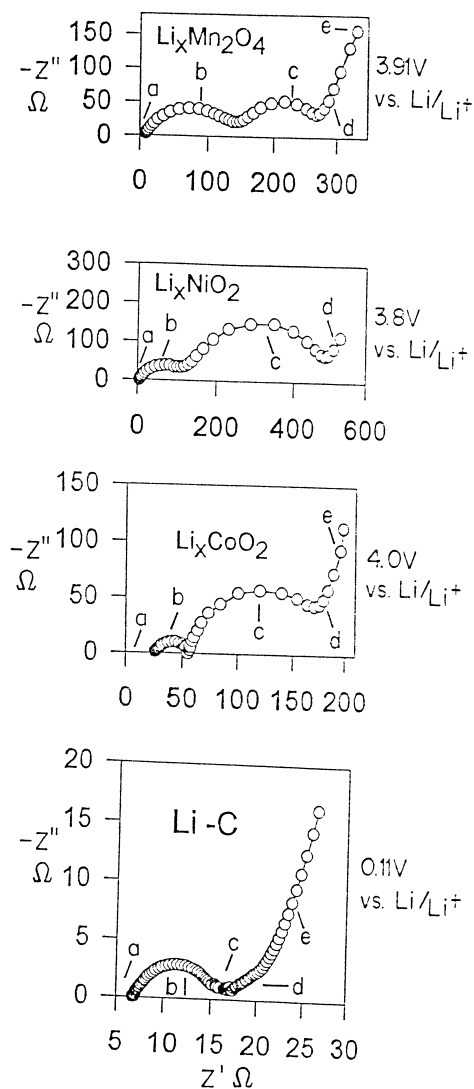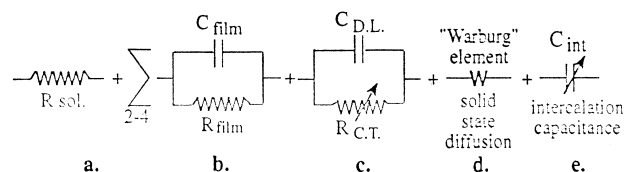

Fig. 11. Typical impedance spectra measured from $LiNiO_2$, $LiCoO_2$, $LiMn_2O_4$ and lithiated graphite electrodes in EC-DMC/$LiAsF_6$ solutions (Li R.E. and C.E. electrodes). The potential of the measurements is indicated near each spectra. A model that provides an excellent fit with these spectra is also presented. The assignment of its various elements to features of the experimental spectra is also shown.

semicircle. It should be noted that as the electrode is thinner and the platelet particles more horizontally oriented (parallel to the current collector), this semicircle is smaller. For ultrathin electrodes (submicronic thickness) this feature does not exist. (c) At the very low frequencies, the
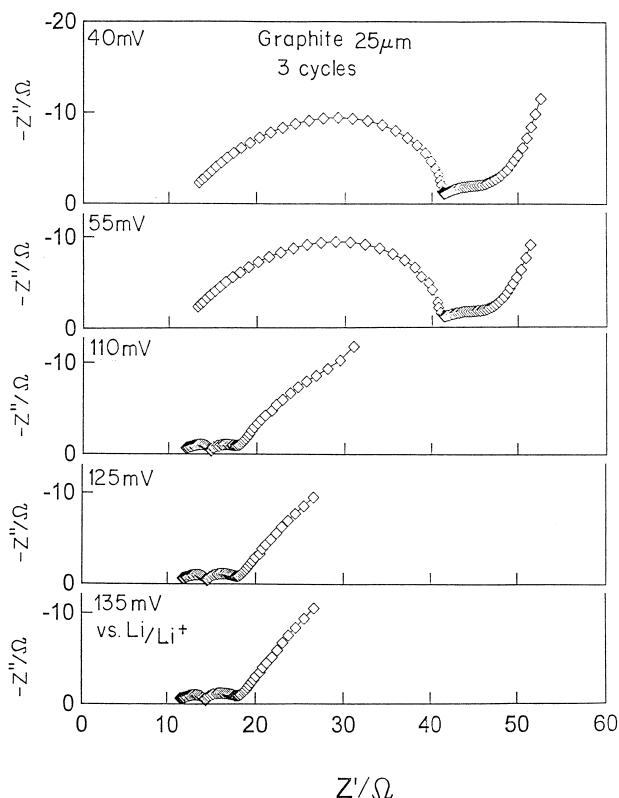
Fig. 12. Impedance spectra measured with a Li–graphite electrode after 3 cycles at different potentials (indicated) in EC-DMC/LiAsF$_6$ 1 M solution. Average particle size 25 μm, 10% PVDF binder (by weight), electrode thickness = 100 μm (a copper grid was used as a current collector).

spectra become a straight line and behave as a Warburg-type element. (d) At the lowest frequencies (mHz region) the spectra become steep lines. The thinner and more oriented the electrodes, the more the steep line changes to a vertical one at the very low frequencies.

(2) The spectra are strongly potential dependent. At the highest intercalation levels (Li$_x$C$_6$ X > 0.5) the high frequency semicircle increases. This increase, however, is reversible and this semicircle contracts upon deintercalation (Fig. 12). We attribute this semicircle to Li ion migration through the surface films that cover Li–graphite electrodes in solutions [8]. Hence, the increase in the semicircle (Fig. 12) is not due to irreversible changes in the surface films' structure occurring at low potentials. We speculate that the increase in the high frequency impedance at the low potentials shown in Fig. 12 is due to an interfacial phenomenon in the boundary between the surface films and the active mass (e.g., increase in Li ion concentration).

(3) We attribute the low frequency semicircle to charge transfer which is related to the interparticle contact. We reached this conclusion because of the strong dependence of this feature on the physical structure (geometry, morphology) of the electrodes.

(4) It is important to note that the Li chemical diffusion coefficient (D) calculated from the Warburg region of the impedance spectra is almost identical to that calculated from PITT. D is strongly potential dependent and has three distinctive minima around 200 mV, 110 mV and 80–70 mV vs. Li/Li$^+$ when calculated during intercalation, and also three minima around 100 mV, 130 mV and 220 mV (Li/Li$^+$) when calculated during deintercalation. It is important to note that at these potentials the intercalation capacity is maximal (appears as peak currents in the slow scan rate cyclic voltammograms). This phenomenon relates to the fact that Li intercalation into graphite involves phase transition and attractive interactions between intercalation sites. The larger the particle size the higher the values of D (along the entire potential domain of interest, 0–300 mV vs. Li/Li$^+$).

(5) Upon cycling, the impedance of the electrodes increases (see Figs. 12 and 13). This is due to microexfoliation of the graphite particles resulting from the repeated intercalation–deintercalation cycling. This microexfoliation gradually increases the surface area of the electrodes, and thus enables continuous reduction of solution species at a small scale (at low potentials). Hence, the electrodes become more extensively covered by an interphase which is composed of surface species–solution reduction prod-
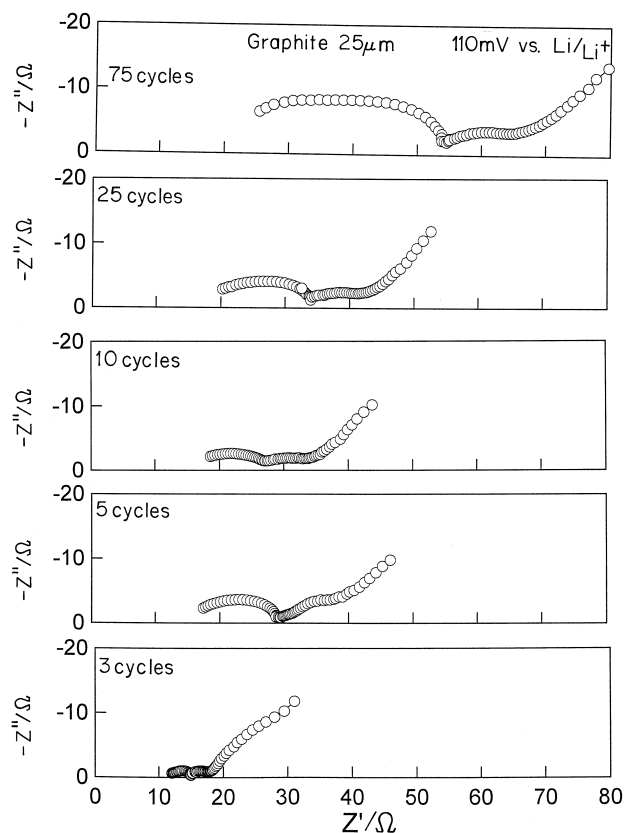

Fig. 13. Impedance spectra measured with an electrode and solution as for Fig. 12 upon cycling at 110 mV (vs. Li/Li$^+$). The cycle numbers are indicated.
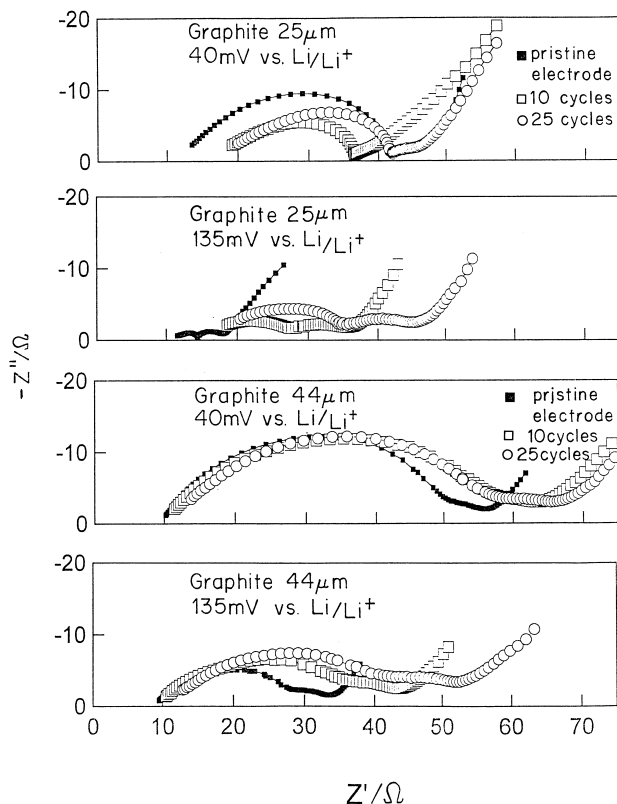
Fig. 14. Impedance spectra measured from Li–graphite electrodes after different cycles and at different potentials, as indicated. Results from two electrodes are compared, 25 and 44 μm average particle size, as indicated. EC-DMC/LiAsF$_6$ solutions, 10% PVDF binder, Cu grid current collector, electrode thickness ≈ μm.

ucts and carbon dust (exfoliated graphite). We can conclude that graphite electrodes fail during prolonged cycling *not* because of major destruction of their active mass, but rather due to a pronounced slow down in their kinetics. This is caused by the increase in their impedance, as described above, and is clearly reflected in Fig. 13.

(6) As the particles are bigger, so the electrode's impedance is higher (Fig. 14). This is due to the fact that as the particles are larger, so the cross-sectional area for Li intercalation per active mass unit is smaller. Hence, for obtaining fast electrodes, small particle size should be used.

It should be emphasized that similar conclusions are also relevant to many types of cathodes used in Li ion batteries.

4. Conclusion

The use of Li metal anodes in rechargeable batteries requires specific surface chemistry and morphology. The electrodes must be covered by highly uniform, elastic surface films which can accommodate the changes in the electrode's surface area upon Li deposition and dissolution. Such a situation occurs in only a very few systems,

including 1–3 dioxolane-based liquid solutions and some gel electrolytes.

In the case of lithiated carbon electrodes, the formation of passivating films is also essential for obtaining prolonged cycle life. However, the requirements for passivation properties and uniformity is less severe than for Li metal electrodes. In electrolyte solutions in which Li$_2$CO$_3$ or (CH$_2$OCO$_2$Li)$_2$ (major EC reduction product) are formed as surface species, lithiated graphite anodes are highly reversible and can undergo prolonged cycling. However, the cycle life of lithiated graphite anodes is limited even in the best solutions due to gradual and inevitable irreversible processes. These include continuous microexfoliation of the active mass which leads to instability of the electrodes' passivation and thus, to continuous reduction of surface species on a small scale at low potentials. Thus, the electrode's impedance continuously and gradually increases during prolonged cycling. It appears that many types of cathodes for Li ion batteries, including Li$_x$CoO$_2$, LiNiO$_2$ and LiMn$_2$O$_4$ are also covered by surface films through which Li ions have to migrate to the active mass.

From many points of view, the electrochemical behavior of these cathodes is similar to that of Li–C electrodes. These include the impedance behavior, the potential dependence of the Li chemical diffusion coefficient and the capacity fading mechanisms. One of the sources for the surface films on the cathode is surface species formed on the anode side which saturate the solutions and reprecipitate on the cathode. The commonly used alkyl carbonate solutions are oxidized on noble metals at potentials below 4 V (Li/Li$^+$). However, it appears that on the cathode materials, these oxidation processes are not pronounced, probably due to the surface films which cover the cathodes.

Acknowledgements

References

[1] D. Aurbach, I. Weissman, A. Zaban, E. Mengeritski, P. Dan, J. Electrochem. Soc. 143 (1996) 2100.
[2] S. Hussain, Handbook of Batteries, 2nd edn., in: D. Linden (Ed.), Rechargeable Lithium Batteries, Chap. 36, McGraw-Hill, New York, 1994.
[3] E. Goren, O. Chusid, D. Aurbach, J. Electrochem. Soc. 138 (1991) L6.
[4] D. Aurbach, B. Markovsky, A. Schechter, Y. Ein-Eli, H. Cohen, J. Electrochem. Soc. 143 (1996) 3809.
[5] D. Aurbach, Y. Cohen, J. Electrochem. Soc. 144 (1997) 3355.
[6] D. Aurbach, Y. Ein-Eli, J. Electrochem. Soc. 142 (1995) 1746.
[7] M.D. Levi, D. Aurbach, J. Electroanal. Chem. 421 (1997) 7989.
[8] D. Aurbach, M.D. Levi, J. Phys. Chem. B 101 (1997) 4630.

[9] D. Aurbach, M. Moshkovich, J. Electrochem. Soc. 145 (1998) 2629.

[10] D. Aurbach, A. Zaban, J. Electrochem. Soc. 141 (1994) 1808.

[11] D. Aurbach, M.D. Levi, E. Levi, B. Markovsky, G. Salitra, H. Teller, U. Heider, V. Hilarius, J. Electrochem. Soc. 145 (1998) 3024.

[12] J. Yamaki, J. Power Sources 20 (1987) 3.

[13] J. Yamaki, S. Tobishima, Y. Sakurai, K. Saito, K. Hayashi, J. Appl. Electrochem. 28 (1998) 135.

[14] K.M. Abraham, T.N. Nguen, R.J. Hurd, G.L. Holleck, A.C. Macrides, Proceedings of the 3rd International Rechargeable Battery Seminar, Deerfield Beach, Fla, March 5–7, 1990. Shawmco, Tulsa, OK, USA, 1990.

[15] D. Aurbach, Y. Ein-Eli, A. Zaban, J. Electrochem. Soc. 141 (1994) L1.

[16] T. Osaka, T. Momma, Y. Matsumoto, Y. Uchida, J. Electrochem. Soc. 144 (1997) 5.

[17] S. Genies, R. Yazami, J. Garden, J.C. Frison, Synthetic Metals 93 (1998) 77.

[18] T. Osaka, T. Homma, T. Momma, H. Yarimizu, J. Electroanal. Chem. 421 (1997) 143.

[19] D. Aurbach, A. Schechter, B. Markovsky, Y. Ein-Eli, V. Koch, J. Electrochem. Soc. 143 (1996) L273.

[20] Y. Ein-Eli, S.F. McDevitt, B. Markovsky, A. Schechter, D. Aurbach, J. Electrochem. Soc. 144 (1997) L80.